AIMS Energy, 11(1): 156–170.
DOI: 10.3934/energy.2023009
Received: 18 October 2022
Revised: 30 January 2023
Accepted: 15 February 2023
Published: 22 February 2023

http://www.aimspress.com/journal/energy

Research article

Effect of piston geometry design and spark plug position on the engine performance and emission characteristics

Quoc Dang Tran[1], Thanh Nhu Nguyen[2] and Vinh Nguyen Duy[3,*]

[1] School of Mechanical Engineering, Hanoi University of Science and Technology, Hanoi, Vietnam
[2] Faculty of Automotive Engineering Technology, Dai Nam University
[3] Faculty of Vehicle and Energy Engineering, Phenikaa University

* **Correspondence**: Email: vinh.nguyenduy@phenikaa-uni.edu.vn; Tel: +89985814118.

Abstract: This paper investigates the influence of piston geometry design and spark plug position on the engine performance and emission characteristics at a range of speeds from 1200 rpm to 2200 rpm. Accordingly, the parameters of the indentation depth, the spark plug position, the location of the recess, and the engine's compression ratio are changed and evaluated. The concave center depth improved the mixture of air and fuel, increased power, and reduced fuel consumption. The power can be improved by up to 3% when the piston top recess is 25 mm. In addition, within a limited range, the combustion process and the engine's power and emission characteristics are enhanced when the engine's compression ratio rises. Increasing the depth of the depression on the top of the piston improves fluid flow in the cylinder, resulting in increased power, fuel efficiency, and emissions; however, the improvement between the indentations remains unclear.

Keywords: combustion chamber geometry; squish flow; center-bowl; converted CNG engine; piston bowl geometry

1. Introduction

The world's natural gas reserves are considered one of the promising energy sources that can meet the needs of diversifying fuel sources and lowering emissions in the transportation sector. However, when using natural gas as a fuel for internal combustion engines, it is necessary to solve a challenging problem such as burning natural gas much more slowly than petroleum-based fuel. Combustion in an internal combustion engine comprises many incredibly complex fuel oxidation processes and chemical reactions that quickly release heat and generate new compounds. The combustion process in an internal combustion engine is highly dependent on characteristics such as temperature, pressure, chemical kinetics, and refrigerant flow within the engine cylinder. The movement of gas within the cylinder of an internal combustion engine is characterized by a turbulent flow and a very complex change in kinetic energy. Changes in the kinetic energy of this fluid are primarily determined by characteristics such as the intake port cross-section, piston travel speed, and combustion chamber shape [1,2]. Initially, the kinetic energy of the fuel-air combination will increase steadily at the end of the intake phase, and it will rapidly decrease when the piston has traveled roughly a third of the compression stroke [3].

Nevertheless, as the engine piston continues to move toward the top dead center (TDC), kinetic energy will increase very quickly for the remainder of the compression stroke. When the piston continues to travel towards the top dead center during the compression stroke, the gas stream's kinetic energy and temperature will increase dramatically compared to the intake process [4]. To take advantage of this benefit and to adequately prepare for the combustion process, it is required to have a piston with the proper form to guide the gas flow to the fire source with the appropriate concentration and diffusion intensity during the combustion process [5,6]. With a proper diffusion intensity, the number of chemicals participating in the redox reaction will rise, resulting in a shorter time required to ignite the fuel intake in the engine cylinder and a reduction in heat loss to the combustion chamber [7]. The diffusion intensity of the gas stream is measured by the turbulence intensity (u), with the diffusion burning rate increasing as the turbulence intensity rises. As a result, the quantity of heat emitted per unit of time can be significantly increased. Still, if the amount of heat transported to the walls of the combustion chamber can be regulated, the engine's thermal efficiency is enhanced dramatically. However, the above studies were only performed on fixed piston top design without addressing its shape's influence on the airflow movement.

Several academics have recently examined the numerous applications of natural gas in internal combustion engines, emphasizing performance, combustion, and exhaust gas emissions. Natural gas has traditionally been used in spark ignition (SI) engines due to its low self-ignitability [8]. This technological approach was used to replace the gasoline engine in several cars because of the reduced cost and emissions [9]. Nonetheless, Ogawa et al. noted that the benefits of natural gas would not be fully explored in SI engines and that the drop in engine power performance was significant [10]. The dual-fuel operating mode of natural gas paired with high reactivity fuel (e.g., diesel fuel) presents a fresh possibility and application mode for CI engines [11]. The micro-pilot diesel was fed into the cylinder under high compression ratio circumstances to ignite the premixed natural gas. Due to the difference in the combustion characteristics of gasoline and CNG fuel, the design of spark-plug placement should also be considered when converting CNG fuel. This issue has not been addressed in the above studies.

The combustion chamber's shape significantly impacts the flow field within the cylinder of direct injection engines. As the primary geometrical parameters, the effects of the piston head, cylinder head,

and injector placement should be explored. A slight change in shape can significantly affect the mixture's distribution within the cylinder. Several have investigated the effect of combustion chamber geometry on the in-cylinder flow field and mixture preparation studies [12–15]. Multi-dimensional modeling with an emphasis on turbulence modeling has been conducted [16,17], and the evolution of gas jet injection has been explored [18]. The influence of piston head form on fluid flow, combustion, and emissions in gas-powered engines has been examined in [13,14]. Data suggest that bowl-in-piston arrangements for piston head shape may be advantageous in natural gas-powered engines. Due to the considerable effect of geometry on the flow field, the optimal flow field and jet development inside the cylinder cannot be attained unless the injector-chamber designs are evaluated in tandem. Huang et al. conducted experiments on natural gas injection and combustion properties in various injector-chamber configurations utilizing a fast compression machine and a natural gas-powered engine. Accordingly, the effects of CNG and gasoline fuels on engine performance and emissions in a dual sequential spark ignition engine were investigated in [19]. The tests and analyses were performed at specified low and high load conditions for gasoline and CNG by varying the engine speed [20]. However, the effect of piston head shapes on engine emissions when running with petrol and CNG fuel has not been thoroughly evaluated.

In this study, structural parameters will be changed, such as depth of indentation on piston top (Hb), the position of piston top concave center position and position of spark plugs relative to cylinder centerline, early ignition angle on software base Avl boost, and experimental evaluation. As a result, this research will clarify the role of the above parameters on the engine characreristics to describe how to find suitable parameters for the engine. The project's research results are an essential basis for optimizing the parameters of diesel engines when switching to CNG fuel.

2. Engine characteristic research methodology

The test engine model was made using the AVL BOOST program described in Figure 1 and Table 1. Theoretical backgrounds, including the basic equation and calculation models for all model components, are mentioned as follows.

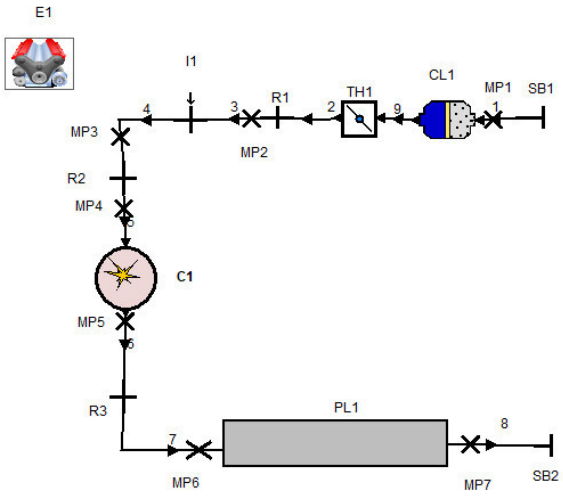

Figure 1. AVL BOOST numerical simulation model of the test engine.

Table 1. Some elements of the simulation models.

No.	Element name	Symbol
1	Intake, Exhaust pipe	-
2	Boundary elements	SB
3	Plenum	PL1
4	Cylinder	C1
5	Restriction	R
6	Measuring point	MP
7	Air cleaner	CL
10	Air cooler	CL

2.1. Basic conservation equations

The first rule of thermodynamics is the foundation for the governing equations of the simulation model. According to Eq (1), the first rule of thermodynamics for a high-pressure cycle state that the piston work, fuel heat input, wall heat losses, and the enthalpy flow due to blow-by are added together to get the change in internal energy in the cylinder:

$$\frac{d(m_C.u)}{d\alpha} = -p_C.\frac{dV}{d\alpha} + \frac{dQ_F}{d\alpha} - \sum\frac{dQ_W}{d\alpha} - h_{BB}.\frac{dm_{BB}}{d\alpha} \tag{1}$$

From the total of the cylinder's inflowing and outflowing masses, we can determine the variation in mass:

$$\frac{dm_C}{d\alpha} = \sum\frac{dm_i}{d\alpha} - \sum\frac{dm_e}{d\alpha} - \sum\frac{dm_{BB}}{d\alpha} + \sum\frac{dm_{ev}}{dt} \tag{2}$$

where m_c, u, p_c, V, Q_F, Q_W, α, h_{BB}, m_{BB}, d_{mi}, d_{me}, m_{ev} represent the mass in the cylinder, specific internal energy, cylinder pressure, cylinder volume, fuel energy, wall heat loss, crank angle, enthalpy of blow-by, blow-by mass flow, mass element flowing into the cylinder, mass element flowing out of the cylinder, and mass of the evaporating fuel, respectively.

2.2. Combustion model

This simulation predicted the combustion characteristics of direct-injection compression ignition engines by using the mixing-controlled combustion (MCC) model. As stated in Eq (3), the heat release is a function of the available fuel amount *(f1)* and the turbulent kinetic energy density *(f2)*:

$$\frac{dQ}{d\phi} = C_{Comb}\cdot f_1(M_F, Q)\cdot f_2(k, V) \tag{3}$$

where ; $f_1(M_F, Q) = M_F - \frac{Q}{LVC}$; $f_2(k, V) = \exp(C_{rate}\cdot\frac{\sqrt{k}}{\sqrt[3]{V}})$, C_{Comb} is the combustion constant, C_{rate} is the constant for mixing rate, k is the local density of turbulent kinetic energy, MF is the mass of vaporised fuel,

LCV is the lower heating value, and *Q* is the cumulative heat release for mixture-controlled combustion, and *V* is the cylinder volume.

2.3. Heat transfer model

The heat transfer to the walls of the combustion chamber, the cylinder head, the piston, and the cylinder is calculated from Eq (4).

$$Q_{wi} = A_i \cdot \alpha_i \cdot (T_c - T_{wi}) \tag{4}$$

Q_{wi}, i, Ai, Tc, T_{wi} represent the wall heat flow, surface area, heat transfer coefficient, Tc gas temperature in the cylinder, and wall temperature, respectively.

Typically, the heat-transfer coefficient is calculated using the Woschni model, which was established in 1978 for high-pressure cycles and may be summarised as follows:

$$\alpha_w = 130.D^{-0.2}.p_c^{0,8}.T_c^{-0.53}.[C_1.c_m + C_2.\frac{v_D.T_{c1}}{p_{c,1}.V_{c,1}}.(p_c - p_{c,0})]^{0.8} \tag{5}$$

where C_1 = 2.28 + 0.308**cu*/c_m; C_2 = 0.00324 for direct-injection engines, *D* is the cylinder bore, c_m is the mean piston speed, c_u is the circumferential velocity, V_D is the displacement per cylinder, $p_{c,o}$ is the cylinder pressure of the motored engine, $T_{c,1}$ is the temperature in the cylinder at the intake valve closing (IVC) and $p_{c,1}$ is the pressure in the cylinder.

2.4. Model control

In this research, to consider the influence of piston top structure, spark plug position, and concave center position on the performance of the converted CNG engine, the simulation is conducted as follows:

- The test engine speed was operated at constant speeds ranging from 1000 rpm to 2000 rpm with 200 rpm increment.
- The quantities of fuel supplied (G_{nl}) and the injection pressure on the intake manifold (p_f) were kept constant with values of 0.755 (g/s) and 1 bar, respectively.
- The diameter of the concave center was kept constant at the value D_b = 60 mm. However, the indentation depth on the piston top (Hb) was changed from 0 to 25 mm with a 5 mm increment. Furthermore, the eccentricity between the spark plug and the cylinder was also changed from 1 to 6 mm with a 1 mm increment.

2.5. Experimental apparatus

Figure 1 depicts a schematic overview of the experimental setup. Natural gas is stored in a bomb with a pressure of around 150 bar before passing through two pressure regulators to reduce the pressure to 50 bar and 4 bar. An MFC/MFM device regulates the engine's natural gas supply, and a manometer monitors the airflow rate. The converted CNG engine is an agricultural diesel engine with a single cylinder adapted for the experiment.

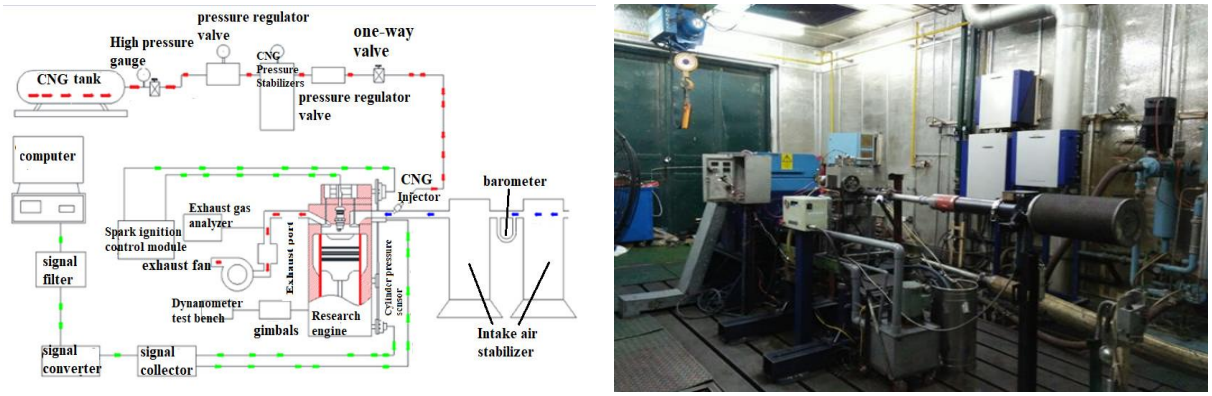

Figure 2. Schematic of the experimental setup.

The CNG injector is situated near the intake valve on the intake pipe. In addition, the spark plug is installed instead of the diesel injector. The testing equipment consists of a chassis dynamometer and a gadget for measuring fuel usage. All devices are operated directly from a computer using specialized software and synchronized and linked to a local network. The chassis dynamometer comprises an absorption unit and tools for measuring torque and rotational speed. Therefore, engine speed and power may be regulated and tested at the rated power of 220 kW, and the rated maximum rotational speed is 4500 rpm. The dynamometer is operated by a PUMA computer collecting inputs from sensors mounted on the test engine. In addition, to verify the correctness of the experimental test, we used AVL 533, an external cooling system that permits continuous temperature control. The Fuel Balance AVL 733S fuel-consumption measuring device measures the amount of fuel based on the gravimetric approach. The fuel system AVL Fuel Balance offers high-precision monitoring of fuel use, even at low usage and in a short amount of time. The equipment's suggested measurement range is up to 150 kg/h with an accuracy of 0.1%.

Furthermore, a specialized sensor is installed in the cylinder head to record the cylinder pressure fluctuation concerning crank angles to determine the specified parameters. This sensor consists of a high-precision AVL piezoelectric pressure transducer and a Kistler 2613B-GU12P crank angle encoder with the specifications shown in Table 2. In addition, many subsystems, including an oil system, a regulating engine unit, intake and exhaust systems, and the data gathering system, have been used to calibrate and regulate engine performance. The parameters of the test engine are shown in Table 3.

Due to the selection of instruments, state of the instrument and laboratory, calibration of equipment, climatic conditions, manual observation, and measurement of readings, errors and uncertainties occur naturally. Risks and faults are associated with the test equipment's physical quantity. The measurements' relative uncertainties were evaluated using the Gaussian distribution to reduce data uncertainty.

Table 2. The specifications of the pressure sensor.

Items	Specifications
AVL piezoelectric pressure transducer	
Measuring range	0–250 bar
Sensitivity	19 pC/bar
Natural frequency	~ 160 kHz
Acceleration sensitivity	≤ 0.0005 bar/g
Insulation resistance	$\geq 10^{13}$ at 20 ℃
Thermal sensitivity change	≤ 1%
Load change drift	1.5 mbar/ms
Weight	
Linearity ≤ ± 0.3% FSO	≤ ± 0.3% FSO

Table 3. The specifications of the converted engine.

Items	Specifications
Engine type	Port injection CNG engine
Bore x stroke (mm)	100 × 115
Compression ratio, ε	11.5 & 12.5
The shape of the piston head	Bowl in piston head (Piston bowl)
Cooling system	Water-cooled with pump
Fuel	CNG

3. Results and discussions

3.1. Simulation model validation

This research contrasts the simulation and experimental findings to validate the model with the same boundary conditions. This study chose to test the engine's working range from 1200 rpm to 2200 rpm because this is the stable working range of the engine recommended by the manufacturer.

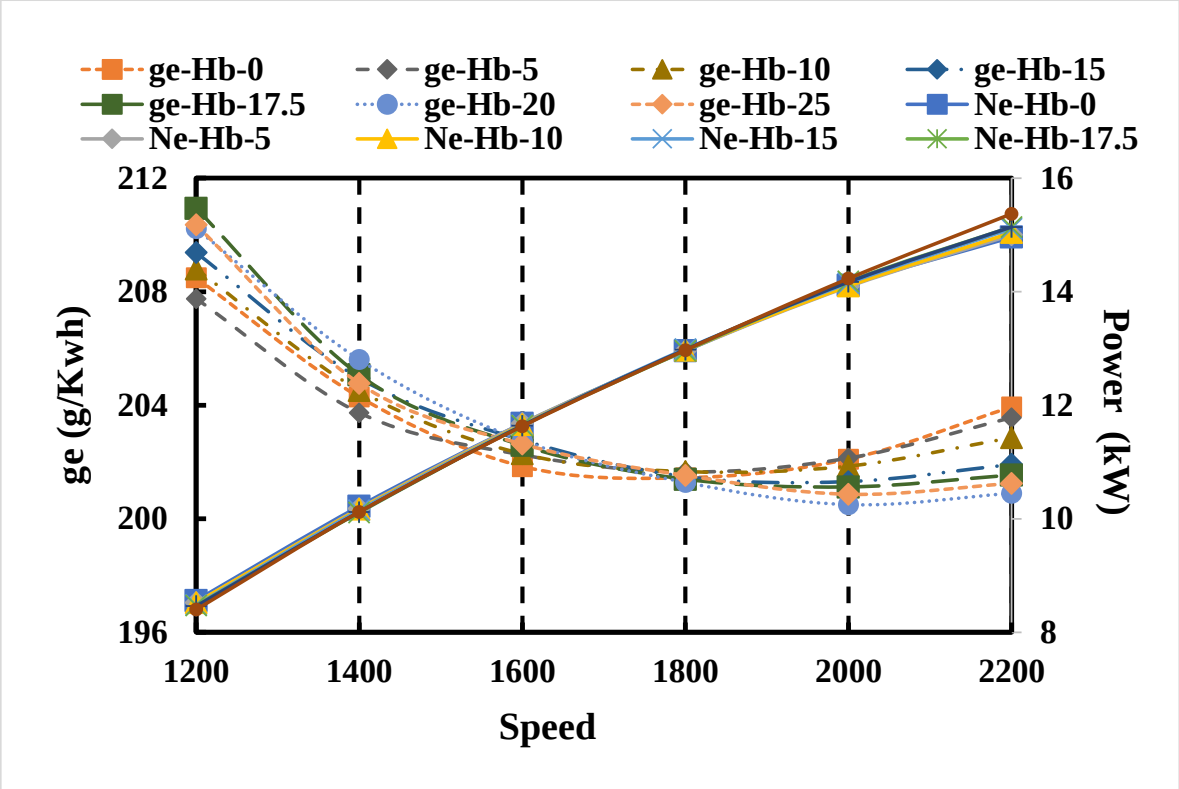

Figure 3. Comparison of engine performance curves between simulation and experimental results.

Figure 3 shows the engine performance of the experimental and simulation data. The solid lines are the test results of the real engine obtained on the engine test bench; meanwhile, the dashed lines are the results obtained from the simulation model after recalibrating the model according to the real conditions. The largest power deviation, 4% (between the simulation and experiment), is observed at 1000 rpm, and the smallest power deviation, 1%, is observed at 2000 rpm. The simulation process's underlying assumptions can be blamed for a slight discrepancy between the simulated and experimental findings. However, in the trials, these presumptions cannot be controlled. In addition, it is challenging to replicate many significant operational and physicochemical parameters of the simulation models in their true values. The simulated outcomes are nonetheless helpful for engine development and research.

3.2. Effect of the recessed piston depth on the engine performance and emission characteristics

Figure 4 shows the effect of piston concave center depth on the test engine performance corresponding to the compression ratio $\varepsilon = 10$, air-fuel ratio $\lambda = 1$), concave center depth $D_b = 60$ (mm), and engine speed varying from n = 1200–2200 rpm. The results with solid lines represent the variation of power, and the broken lines are the results of the variation in fuel consumption. It can be observed that the power and fuel consumption do not change dramatically according to the change of the piston concave center depth, especially at engine speeds lower than 2000 rpm. The engine power increases in proportion to the speed; meanwhile, the fuel consumption tends to decrease at lower speeds and reaches the minimum value at n = 1800 rpm. Furthermore, it can also conclude that the concave center

depth improved the mixture of air and fuel and increased power and reduced fuel consumption. As a result, the power can be improved by up to 3% when the piston top recess is 25 mm. As the rotation speed increases, the vortex will also increase, so the influence of the piston's concave center depth on the vortex will be reduced.

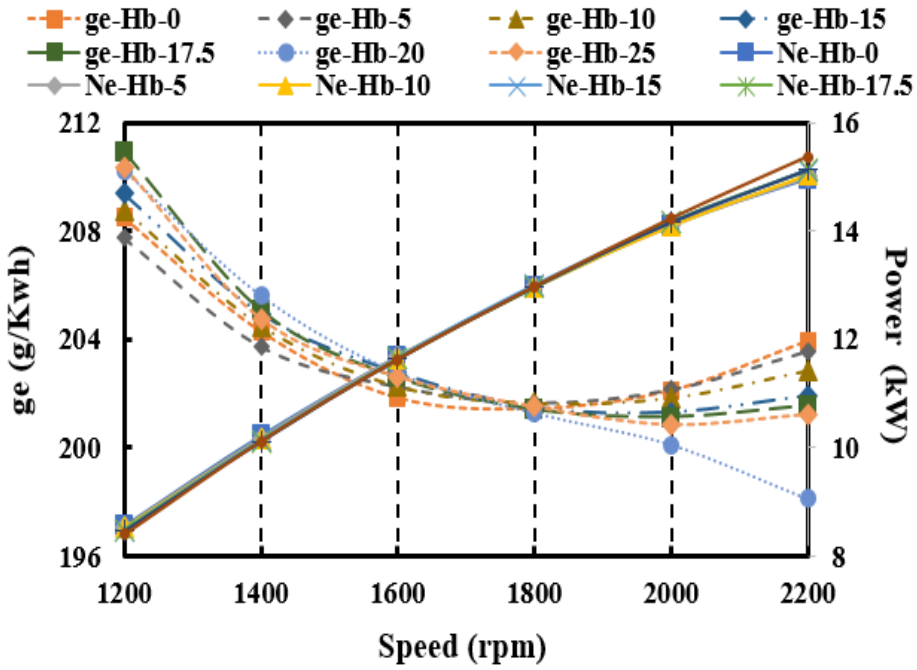

Figure 4. Effect of the concave center depth on power and fuel consumption.

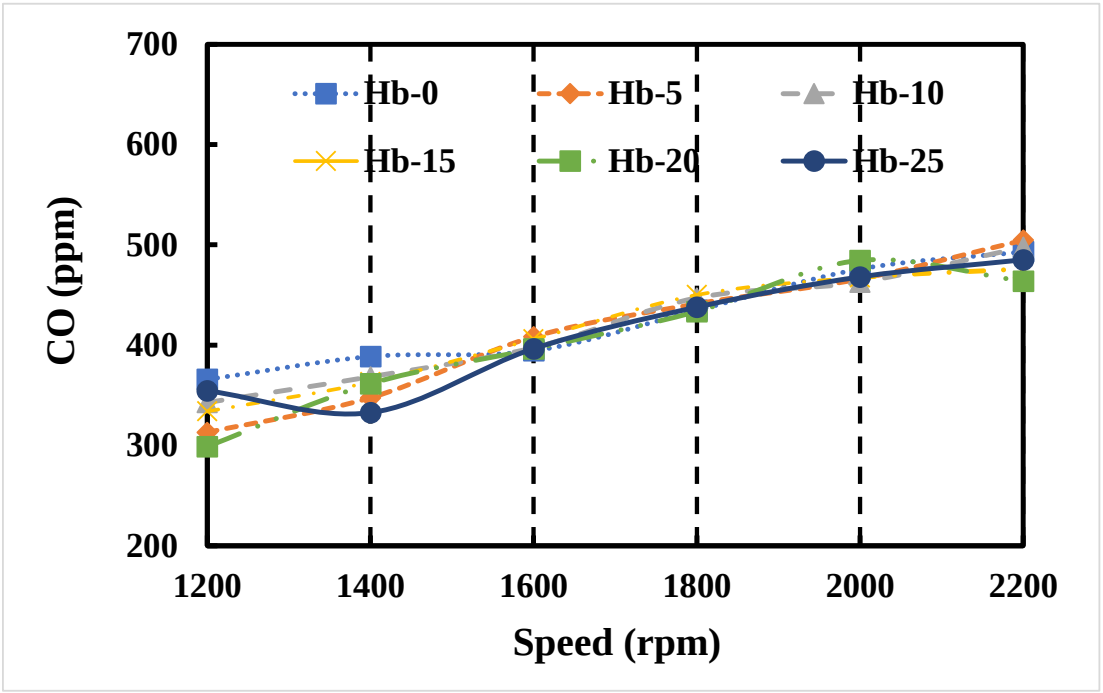

Figure 5. Effect of concave center depth on CO emissions.

Figure 5 describes the CO emissions of the test engine according to the engine speed corresponding to the different piston-recessed peak depths. In general, CO emissions decrease when the engine speed reduces from 1200 to 1400 rpm, increasing significantly in the high engine speed rate. Figure 5 also shows the piston top indentation depth's role in improving combustion and reducing CO emissions. However, this effect is only noticeable at low engine rpm. Even at high speed, when the depth of the piston top recess increases, CO emissions also tend to increase.

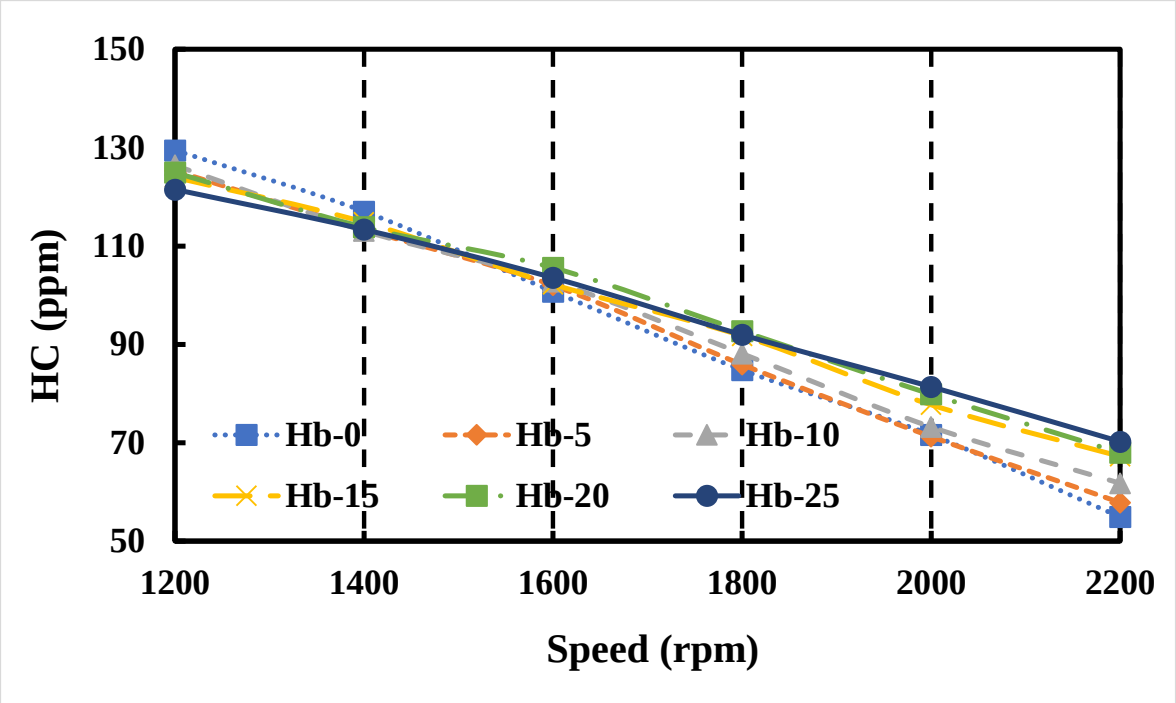

Figure 6. Effect of concave center depth on HC emissions.

Figure 6 Shows HC emissions according to the engine speed for different depths of the piston concave crest. It can be observed that, as a result, in the figure, HC tends to reduce as the engine speed increases. The decrease in HC corresponding to different peak depths of indentation was almost the same during the experiment. As the piston peak depth increases and the engine speed increases, the turbulence speed increases before the top dead center, helping to reduce the combustion time of the mixture and reducing HC emissions. At the engine speed of 2200 rpm, HC emissions are 2.4 times less than those at the engine speed of 1200 rpm.

NOx emissions of the studied engine are shown in Figure 7. Accordingly, NOx emissions tend to decrease with increasing engine speed, and the most significant NOx reduction is at the engine speed of 2200 rpm and concave center depth of 5 mm. The results show that the combustion rate is shortened, and the engine's heat dissipation rate is improved, resulting in less excess air in the combustion process and better cooling of the internal temperature of the combustion chamber by taking advantage of the combustion chambers. The squish flow inside the cylinder and the combustion chamber area in the cylinder are optimized.

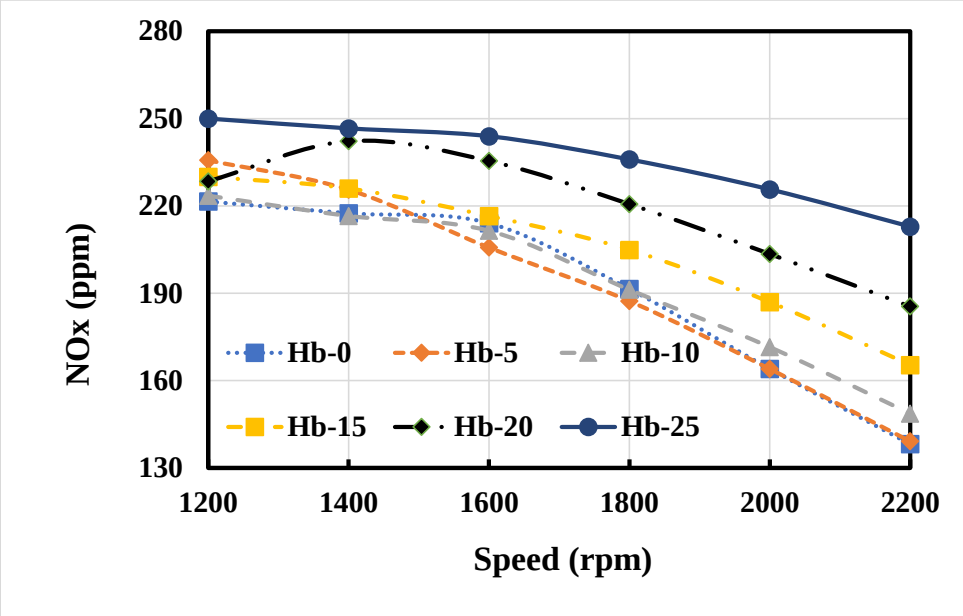

Figure 7. Effect of concave center depth on NOx emissions.

It can be concluded that lower efficiency is caused by the shallow piston bowl design because fuel contacts the cylinder lining at all spray angle values. Such zones allow fuel to reach the cylinder liner; only large engines with a significant distance between the sprayer and the cylinder liner as well as engines with high boosting pressure, benefit from shallow piston bowls because the high air density shortens the spray penetration distance and prevents fuel from reaching the cylinder liner. Deep piston bowls are advantageous if the engine has a low boost pressure and the fuel sprays have a long penetration length because of the low air density and the prolonged injection.

3.3. Effect of spark plug displacement position and concave center position

Figure 8 shows the effect of the concave center position on the test engine's performance and emissions corresponding to various compression ratios. We can see that the engine's compression ratio directly affects performance, fuel consumption, and emissions. Accordingly, when the compression ratio increases, the capacity increases significantly. The engine's fuel consumption is also considerably improved when the compression ratio rises. The emission norms also tend to decrease when the compression ratio increases, especially NOx emission. In addition, when changing the spark plug set point relative to the center position corresponding to the positions of 1, 2, 3, 4, 5, and 6 mm, the evolution of power, fuel consumption, and emissions have also changed markedly. When the spark plug is placed in the center position, the engine power is maximum, and the fuel consumption is minimal; the most significant difference can be up to 3%. This is also a commonly implemented design in practice. However, the HC emission, in this case, tends to increase compared to the spark plug design located far from the center. In contrast, CO emissions fluctuate and peak differently with different engine compression ratios.

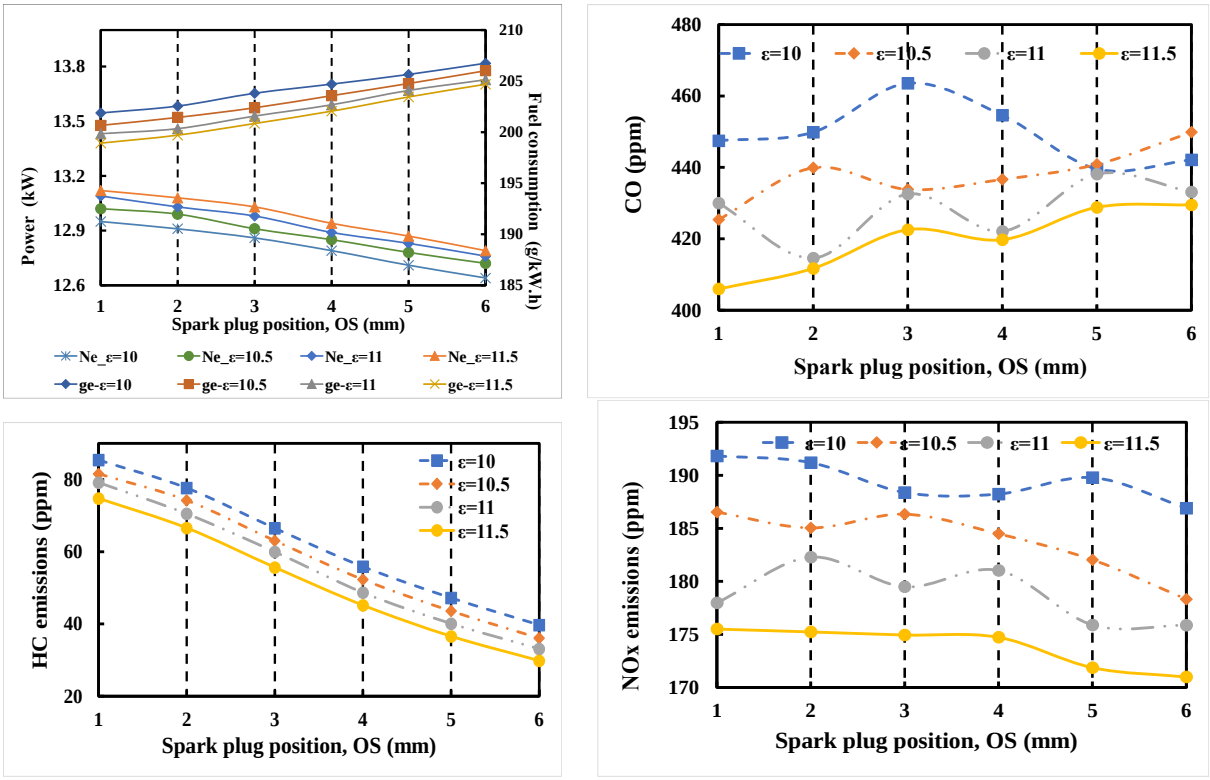

Figure 8. Effect of spark plug displacement position on the test engine's performance and emissions.

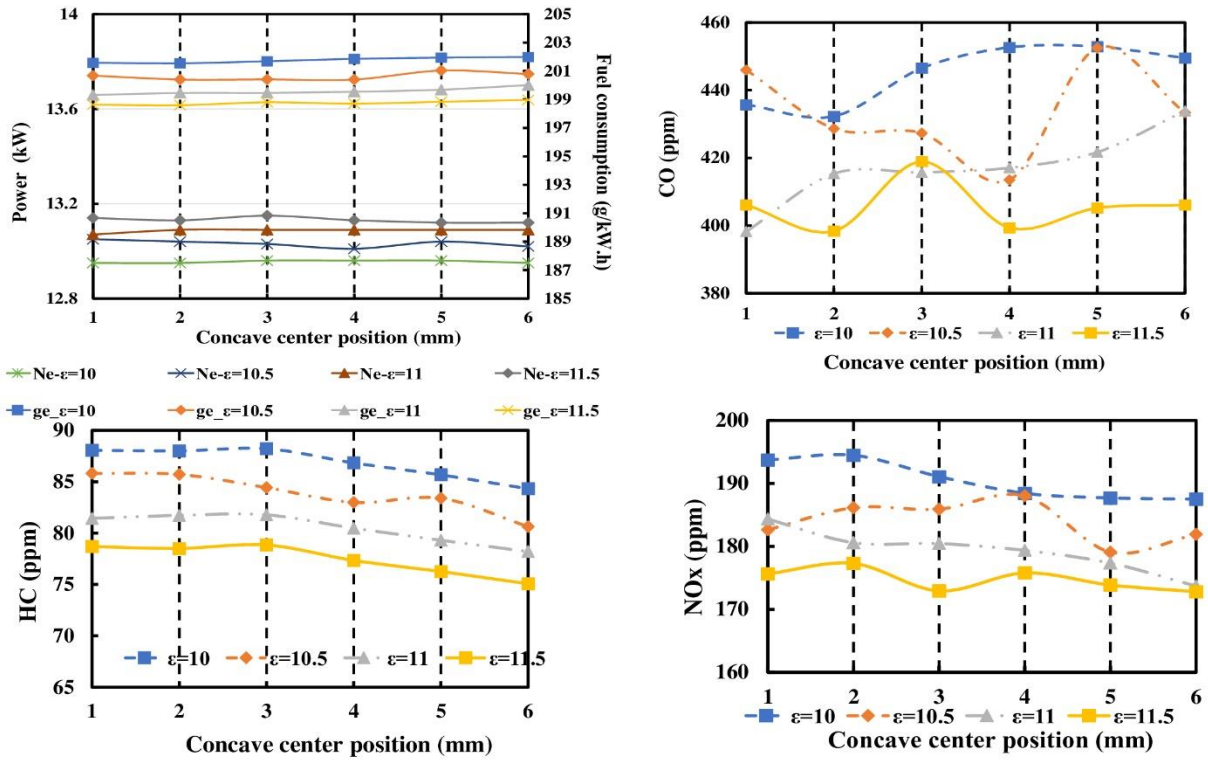

Figure 9. Effect of the concave center position on the test engine's performance and emissions.

Figure 9 shows the effect of the concave center position on the test engine's performance and emissions. Accordingly, the compression ratio still plays an essential role in the engine's power and fuel consumption in all cases where the piston center is concave. However, the influence of the piston on the concave position on the above parameters is insignificant when the power curve and fuel consumption do not change much when changing the position of the concave center. Meanwhile, CO and HC emissions decrease when the concave center position is moved away from the center position. CO emissions fluctuate concerning the concave center positions and the compression ratio variation. Through the above results, we can draw that the influence of the displacement position of the spark plug will be larger than the influence of the compression ratio on the engine, and the influence of the displacement of the concave center will be less than that of the compression ratio to the power, torque, fuel consumption, and emissions.

4. Conclusions

This study analyzes the results obtained from the simulation on the influence of parameters such as depth of concave on top of the piston, concave center position, spark plug placement, and compression ratio on the power performance, fuel consumption, and engine emissions of the test engine. The simulation model is adjusted to evaluate the reliability through comparison with the experiment under the same conditions. Research results show that when the engine's compression ratio increases within a certain limit, it helps to improve the combustion process and improves the engine's power and emission characteristics. Increasing the recess depth on the top of the piston enhances the cylinder's fluid flow, resulting in improved power, fuel consumption, and emissions. Still, the improvement between the indentations is not clear. The effect of the spark plug position will be more significant on the concave center position due to combustion time and uncontrolled kinematics inside the combustion chamber. The detailed chemical kinetic mechanism of the combustion process, the heat release, cylinder pressure, and combustion duration of the engine with various parameters will be performed in future research.

Data availability statement

The authors confirm that the data supporting the findings of this study are available within the article Reference.

Conflict of interest

All authors declare no conflict of interest regarding this paper.

References

1. Nguyen Duc K, Nguyen Duy V, Hoang-Dinh L, et al. (2019) Performance and emission characteristics of a port fuel injected, spark ignition engine fueled by compressed natural gas. *Sustainable Energy Technol Assess* 31: 383–389. https://doi.org/10.1016/j.seta.2018.12.018
2. Jiaqiang E, Pham MH, Deng Y, et al. (2018) Effects of injection timing and injection pressure on performance and exhaust emissions of a common rail diesel engine fueled by various concentrations of fish-oil biodiesel blends. *Energy* 149: 979–989. https://doi.org/10.1016/j.energy.2018.02.053
3. Dinh T, Nguyen K, Pham T, et al. (2020) Study on performance enhancement and emission reduction of used carburetor motorcycles fueled by flex-fuel gasoline-ethanol blends. *J Chinese Inst Eng* 43: 1–12. https://doi.org/10.1080/02533839.2020.1751719
4. Duc KN, Tien HN, Duy VN (2018) Performance enhancement and emission reduction of used motorcycles using flexible fuel technology. *J Energy Inst* 91: 145–152. https://doi.org/10.1016/j.joei.2016.09.004
5. Duy VN, Duc KN, Cong DN, et al. (2019) Experimental study on improving performance and emission characteristics of used motorcycle fueled with ethanol by exhaust gas heating transfer system. *Energy Sustainable Dev* 51: 56–62. https://doi.org/10.1016/j.esd.2019.05.006
6. Cong DN, Duc KN, Nguyen V (2021) The effects of dimethyl ether enriched air (DMEA) on exhaust pollutants and performance characteristics of an old generation diesel engine. *Int J Sustainable Eng* 14: 1143–1156. https://doi.org/10.1080/19397038.2021.1896590
7. Nguyen TD, Tran Anh T, Quang VT, et al. (2020) An experimental evaluation of engine performance and emissions characteristics of a modified direct injection diesel engine operated in RCCI mode. *AIMS Energy* 8: 1069–1087. https://doi.org/10.3934/energy.2020.6.1069
8. Duy V, Duc K, Thanh TN, et al. (2020) Implementation of fuel additive MAZ 100 for performance enhancement of compressed natural gas engine converted from in-used gasoline engine. *J Air Waste Manage Assoc* 70: 932–943. https://doi.org/10.1080/10962247.2020.1781709
9. Shiga S, Ozone S, Machacon HTC, et al. (2002) A study of the combustion and emission characteristics of compressed-natural-gas direct-injection stratified combustion using a rapid-compression-machine. *Combust Flame* 129: 1–10. https://doi.org/10.1016/S0010-2180(01)00367-4
10. Hekkert MP, Hendriks FHJF, Faaij APC, et al. (2005) Natural gas as an alternative to crude oil in automotive fuel chains well-to-wheel analysis and transition strategy development. *Energy Policy* 33: 579–594. https://doi.org/10.1016/j.enpol.2003.08.018
11. Warguła Ł, Kukla M, Lijewski P, et al. (2020) Impact of compressed natural gas (CNG) fuel systems in small engine wood chippers on exhaust emissions and fuel consumption. *Energies* 13. https://doi.org/10.3390/en13246709
12. Usman M, Hayat N (2019) Use of CNG and Hi-octane gasoline in SI engine: a comparative study of performance, emission, and lubrication oil deterioration. *Energy Sources, Part A Recover Util Environ Eff* 1: 1–15. https://doi.org/10.1080/15567036.2019.1683098
13. Hagos DA, Ahlgren EO (2018) Well-to-wheel assessment of natural gas vehicles and their fuel supply infrastructures—Perspectives on gas in transport in Denmark. *Transp Res Part D Transp Environ* 65: 14–35. https://doi.org/10.1016/j.trd.2018.07.018

14. Cho HM, He BQ (2007) Spark ignition natural gas engines—A review. *Energy Convers Manage* 48: 608–618. https://doi.org/10.1016/j.enconman.2006.05.023
15. Gnap J, Dočkalik M (2021) Impact of the operation of LNG trucks on the environment. *Open Eng* 11: 937–947. https://doi.org/10.1515/eng-2021-0096
16. Pourkhesalian AM, Shamekhi AH, Salimi F (2010) Alternative fuel and gasoline in an SI engine: A comparative study of performance and emissions characteristics. *Fuel* 89: 1056–1063.
17. Evans RL, Blaszczyk J (1997) A comparative study of the performance and exhaust emissions of a spark ignition engine fuelled by natural gas and gasoline. *Proc Inst Mech Eng Part D J Automob Eng* 211: 39–47. https://doi.org/10.1016/j.fuel.2009.11.025
18. Yontar AA, Doğu Y (2018) Experimental and numerical investigation of effects of CNG and gasoline fuels on engine performance and emissions in a dual sequential spark ignition engine. *Energy Sources, Part A Recover Util Environ Eff* 40: 2176–2192. https://doi.org/10.1080/15567036.2018.1495783
19. Jahirul MI, Masjuki HH, Saidur R, et al. (2010) Comparative engine performance and emission analysis of CNG and gasoline in a retrofitted car engine. *Appl Therm Eng* 30: 2219–2226. https://doi.org/10.1016/j.applthermaleng.2010.05.037
20. Yontar AA, Doğu Y (2018) Investigation of the effects of gasoline and CNG fuels on a dual sequential ignition engine at low and high load conditions. *Fuel* 232: 114–123. https://doi.org/10.1016/j.fuel.2018.05.156

AIMS Press